ARCHIVE OF MECHANICAL ENGINEERING

DOI: 10.24425/ame.2022.143096 2022, Vol. 69, No. 4, pp. 615–628

Riyah N. KITER[1], Mazin Y. ABBOOD[1], Omar H. HASSOON[2]

Modeling of the axial crumpling of conical shells

Received 29 November 2021, **Revised** 1 July 2022, **Accepted** 25 September 2022, **Published online** 15 November 2022

Keywords: axial crushing, concertina, eccentricity, ABAQUS, inward folding

The axial crumpling of frusta in the axisymmetric "concertina" mode is examined. A new theoretical model is developed in which the inward folding in both cylinders and frusta is addressed. The results were compared with previous relevant models as well as experimental findings. The flexibility of the model was substantiated by its capability of describing and estimating the inward folding in frusta in general as well as in cylinders as a special case. A declining trend of the eccentricity dependence with the D/t ratio was found in contrast with a previous theory which suggests total independency. ABAQUS 14-2 finite element software was employed to simulate the thin tube as a 3-D thin shell part. Numerical simulations of the process were found to, firstly, underestimate the theoretical values of inward folding in general, secondly anticipate more underestimations as the tubes become thinner and/or have larger apex angle, and finally anticipate as low as 300 apical angle frusta to revert its mode of deformation to global inversion.

Nomenclature

D	smaller diameter of frustum
$h_1,\ h_2$	plastic half-wavelengths
h	crushed length
$m_1,\ m_2$	eccentricity factor for h_1, h_2
M_p	fully plastic bending moment per unit length
$\overline{P}$	mean crushing force

✉ Omar H. Hassoon, e-mail: omar.h.hassoon@uotechnology.edu.iq

[1]Department of Mechanical Engineering, College of Engineering, University of Anbar, Iraq. ORCID: (M.A.) 0000-0002-9236-9205

[2]Department of Production and Metallurgy Engineering, University of Technology, Baghdad, Iraq. ORCID: 0000-0002-4695-1894

t	thickness of tube
V	volume of frustum
W_B	energy dissipated due to plastic bending
W_S	energy dissipated due to plastic stretching
x	inward displacement of the fold
y	arbitrary coordinate
Y	tensile yield strength
δ	axial displacement of crushing
α	semi-apical angle of frustum
β	angle of rotation of leg AB
γ	angle of rotation of leg BC

1. Introduction

The crushing of short and right prismatic thin-walled structures is of major interest in the field of energy absorption for their relatively high specific energy of deformation. Different shapes of axisymmetric ductile tubes result in different modes of collapse when axially crushed in quasi-static or dynamic tests. Axisymmetric (or concertina) mode is more likely to occur than a non-symmetric (or diamond) mode in relatively thick tubes undergoing a plastic crumpling process, see Fig. 1.

Fig. 1. Axisymmetric mode of deformation [1]

In this figure, an eccentricity (with reference to the tube generator) relating the inward and outward parts of the folds is evident. When a tube starts to deform into axisymmetric fold, it may revert to a diamond fold as collapse proceeds.

In Alexander [2] analysis, the material is assumed to be rigid perfectly-plastic one. In this analysis, the author postulated three plastic hinges and the region between these hinges are exhibiting plastic circumferential stretching. The wave length of the fold – to be – was obtained by minimizing the external work consumed by one-fold formation. Later, many authors adopted a more realistic mechanism of

folding wherein only outward folding is assumed [3–8]. However, experimental observations confirm that the material is capable of folding to both sides of the original radius of the cylinder. Wierzbicki et al. [9] were the first to account for the inward as well as outward displacement of the tube generator. To achieve that, they developed a model of tube crushing which contains two "Super-folding" elements of equal lengths. The eccentricity parameter has had to be assumed in advance as well as three stationary plastic hinges have to be instantaneously formed. Though arbitrary and indeterminate, the so-called eccentricity factor introduced by Wierzbicki et al. [9] was essential to describe the physical behavior of concertina mode of tube deformation and folding. The load-deflection history has been analyzed and the mean crushing load was estimated as well. Following the arguments of Wierzbicki et al. [9], the eccentricity factor was derived by Singace et al. [10] and values of the critical angles required for the formation of the inward and outward folds obtained from the analysis were substantiated by experiments. Both of works [9, 10] were not valid for the first fold, rather they assumed its existence in advance.

Truncated circular cones (or frusta) are favorable for its stability regarding plastic behavior during axial crushing. An undetailed analysis was carried out by Postlethwaite and Mills [11], which was based on Alexander's method [2]. They reported the formula for the mean crushing force as:

$$\overline{P} = 6Yt\sqrt{t(D + 2\delta \sin\alpha)} + 5.69Yt^2 \tan\alpha \,. \tag{1}$$

Mamalis et al. [12] proposed a theoretical model to predict the energy dissipated and the mean crushing load for thin walled circular frusta deformed in concertina mode. Their model was essentially based on plastic hinge-stretching concept of material deformation. As external and internal convolutions are alternatively formed, the mean crushing load was averaged as:

$$\overline{P} = 6Yt\left(\sqrt{Dt} + 0.95t\tan\alpha\right) \tag{2}$$

and the wave length of convolutions are

$$h_1 = \frac{1 + \sin\alpha}{2\cos\alpha}\sqrt{\frac{2\pi Dt}{\sqrt{3}}}\,, \tag{3a}$$

$$h_2 = \frac{1 - \sin\alpha}{2\cos\alpha}\sqrt{\frac{2\pi Dt}{\sqrt{3}}}\,. \tag{3b}$$

Later on, Mamalis et al. [13] were able to predict the deformation history of the crushing process of frusta as well as cylinders in concertina mode of deformation. Experiments conducted on Aluminum conical frusta by Gupta et al. [14] have revealed the transformation of deformation mode from diamond to rolling and stationary plastic hinges at about 45° semi-apical angle. The inward inversion

of the smaller end and/or the outward inversion of the large end were found by Alghamdi et al. [15] to occur in frusta with 60° semi-apical angle and a few of 45° angles. Mohamed et al. [16] simulated and analyzed the dynamic crushing of thin frusta. They found that the flow stress, thickness and angle have more influence on energy absorption by the shell than the bottom diameter and height of the cones. They argued that as the semi-apical angle decreases, the shell becomes more and more steep and undergoes more deformation and hence more energy is absorbed and as the angle increases the shell undergoes less deformation and hence less energy is absorbed.

To the author's knowledge, no effort was made to describe and quantify the inward radial displacement of the tube generator of conical frusta. Thus, a general and simplified analysis whereby inward folding of conical frusta as well as cylinders is presented in the pages to follow.

2. Analytical model

The axial crushing process is usually performed by flat platens. While the platen exerts only normal forces on the walls of cylinder prior to buckling, both normal and lateral forces are exerted on the walls of a frustum. In view of the oblique loading on the walls of frusta, externally-radial stresses are built up and promoting an inward folding. The kinematics governing the formation of one fold thus requires three moving plastic hinges as well as a three straight link mechanism in order to allow for inward folding, as shown in Fig. 2. In this mechanism, plastic hinges are moving such that the inward displacements AA_1 and CC_1 satisfy the boundary conditions, i.e.,

$$\overline{AA_1} = x \sin\beta\,, \tag{4a}$$

$$\overline{CC_1} = x \sin\gamma\,, \tag{4b}$$

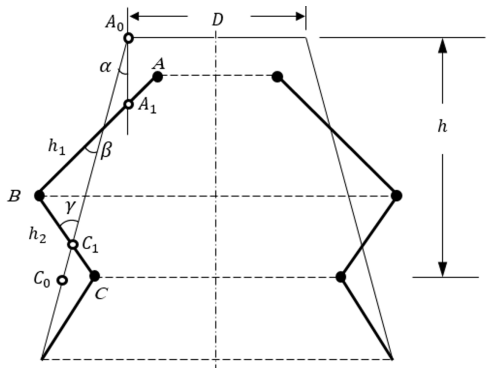

Fig. 2. A modified model of tube collapse

so that at the end of a fold, they will be equal, i.e.

$$\overline{AA_1} = \lim_{\beta \to \frac{\pi}{2} - \alpha} (x \sin \beta) = x \cos \alpha \,, \tag{5a}$$

$$\overline{CC_1} = \lim_{\gamma \to \frac{\pi}{2} + \alpha} (x \sin \gamma) = x \cos \alpha \tag{5b}$$

The energy dissipated due to plastic bending is:

$$W_B = \int_{\beta=0}^{\frac{\pi}{2}-\alpha} \pi \left(D_A + D_B\right) M_p \, \mathrm{d}\beta + \int_{\gamma=0}^{\frac{\pi}{2}+\alpha} \pi \left(D_B + D_C\right) M_p \, \mathrm{d}\gamma \,, \tag{6}$$

where

$$M_p = \frac{Yt^2}{2\sqrt{3}} \,, \tag{7}$$

$$D_A = D - 2x, \sin \beta \sin \left(\beta + \alpha\right) , \tag{8}$$

$$D_B = D + 2 \left(h_1 - x \sin \beta\right) \left(\sin \left(\beta + \alpha\right)\right) = D_C + 2h_2 \sin \left(\gamma - \alpha\right) , \tag{9}$$

$$D_C = D + 2 \left(h_1 + h_2 - x \sin \gamma\right) \sin \alpha - 2x \sin \gamma \sin \left(\gamma - \alpha\right) , \tag{10}$$

$$D_{C_0} = D + 2 \left(h_1 + h_2\right) \sin \alpha . \tag{11}$$

Thus

$$W_B = \frac{\pi Y t^2}{\sqrt{3}} \left[\pi D - x \left\{\pi \cos \alpha + 2 \sin \alpha (1 + \sin \alpha)\right\} + \left(h_1 + h_2\right) \left\{\cos \alpha + (\pi + 2\alpha) \sin \alpha\right\}\right] \tag{12}$$

and the energy dissipated due to stretching, neglecting its effect of thinning of the cross-section, is:

$$W_S = W_s^{AB} + W_s^{BC} \,,$$

$$W_s^{AB} = \int_{y=0}^{h_1} Y e_1(y) \pi \left(D + 2y \sin \alpha\right) t * \mathrm{d}y \,,$$

where:

$$e_1(y) = \lim_{\beta \to \frac{\pi}{2} - \alpha} \left[\frac{\pi \left\{D_B - 2 \left(h_1 - y\right) \sin(\beta + \alpha)\right\}}{\pi \left(D + 2y \sin \alpha\right)} - 1\right] = \frac{2y(1 - \sin \alpha) - 2x \cos \alpha}{D + 2y \sin \alpha} \,. \tag{13}$$

The location at the leg AB, where the strain is reversed, has to be determined by letting

$$e_1(y) = 0$$

so that

$$y = y_1 = \frac{x\cos\alpha}{1-\sin\alpha}\,. \tag{14}$$

Thus

$$\begin{aligned} W_s^{AB} &= \left| \int_{y=0}^{y_1} Ye_1(y)\pi\,(D+2y\sin\alpha)\,t * \mathrm{d}y \right| \\ &\quad + \int_{y=y_1}^{h_1} Ye_1(y)\pi\,(D+2y\sin\alpha)\,t\,\mathrm{d}y \\ &= \pi Yt\left\{h_1^2(1-\sin\alpha) - 2h_1x\cos\alpha + 2x^2(1+\sin\alpha)\right\}. \end{aligned} \tag{15}$$

Similarly

$$W_s^{BC} = \int_{y=0}^{h_2} Ye_2(y)\pi\left(D_{C_0} - 2y\sin\alpha\right)t\,\mathrm{d}y,$$

where

$$\begin{aligned} e_2(y) &= \lim_{\gamma\to\frac{\pi}{2}+\alpha}\left[\frac{\pi\left\{D_C + 2y\sin(\gamma-\alpha)\right\}}{\pi\left(D_{C_0} - 2y\sin\alpha\right)} - 1\right] \\ &= \frac{(1+\sin\alpha)(2y-2x\cos\alpha)}{D_{C_0} - 2y\sin\alpha}\,. \end{aligned} \tag{16}$$

Again, the location at the leg BC, where the strain is reversed, has to be determined by letting

$$e_2(y) = 0.$$

So that

$$y = y_2 = x\cos\alpha. \tag{17}$$

Thus

$$\begin{aligned} W_s^{BC} &= \left| \int_{y=0}^{y_2} Ye_2(y)\pi\left(D_{C_0} - 2y\sin\alpha\right)t\,\mathrm{d}y \right| \\ &\quad + \int_{y=y_2}^{h_2} Ye_2(y)\pi\left(D_{C_0} - 2y\sin\alpha\right)t\,\mathrm{d}y \\ &= \pi Yt(1+\sin\alpha)\left(h_2^2 - 2h_2x\cos\alpha + 2x^2\cos^2\alpha\right). \end{aligned} \tag{18}$$

Summing up, the total energy dissipated in compression or extension is:

$$W_S = \pi Yt\left\{h_1^2(1-\sin\alpha) - 2h_1 x\cos\alpha + 2x^2(1+\sin\alpha) + (1+\sin\alpha)\left(h_2^2 - 2h_2 x\cos\alpha + 2x^2\cos^2\right)\right\}. \tag{19}$$

The energy for plastic dissipation is supplied by the axial compressive force, thus, the mean crushing force is:

$$\overline{P} = \frac{W_B + W_S}{h}, \tag{20}$$

where

$$h = (h_1 + h_2)\cos\alpha. \tag{21}$$

Substituting equations (12), (19) and (21) in Eq. (20)

$$\overline{P} = \frac{1}{(h_1+h_2)\cos\alpha}\left[\frac{\pi Yt^2}{\sqrt{3}}\left\{\pi D - x\left\{\pi\cos\alpha + 2\sin\alpha(1+\sin\alpha)\right\}\right.\right. + (h_1+h_2)\left\{\cos\alpha + (\pi+2\alpha)\sin\alpha\right\}\Big\} + \pi Yt\left\{h_1^2(1-\sin\alpha) - 2h_1 x\cos\alpha + 2x^2(1+\sin\alpha)\right. + (1+\sin\alpha)\left.\left.\left(h_2^2 - 2h_2 x\cos\alpha + 2x^2\cos^2\alpha\right)\right\}\right]. \tag{22a}$$

Using short notation

$$\overline{P} = \frac{C_1 - C_2 x + C_3(h_1+h_2) + C_4 h_1^2 - C_5 h_1 x + C_6 x^2 + C_7 h_2^2 - C_8 h_2 x + C_9 x^2}{h_1+h_2}, \tag{22b}$$

where

$$\begin{aligned}
C_1 &= \frac{\pi^2 Yt^2 D}{\sqrt{3}\cos\alpha}, & C_2 &= \frac{\pi Yt^2}{\sqrt{3}}\left\{\pi + 2(1+\sin\alpha)\tan\alpha\right\},\\
C_3 &= \frac{\pi Yt^2}{\sqrt{3}}\left\{1 + (\pi+2\alpha)\tan\alpha\right\}, & C_4 &= \frac{\pi Yt}{\cos\alpha}(1-\sin\alpha),\\
C_5 &= 2\pi Yt, & C_6 &= \frac{2\pi Yt}{\cos\alpha}(1+\sin\alpha),\\
C_7 &= \frac{\pi Yt}{\cos\alpha}(1+\sin\alpha), & C_8 &= 2\pi Yt(1+\sin\alpha),\\
C_9 &= 2\pi Yt(1+\sin\alpha)\cos\alpha.
\end{aligned} \tag{23}$$

Minimizing the mean crushing force, i.e.,

$$\frac{\partial\overline{P}}{\partial x} = \frac{\partial\overline{P}}{\partial h_1} = \frac{\partial\overline{P}}{\partial h_2} = 0.$$

Thus

$$-C_2 - C_5 h_1 + 2C_6 x - C_8 h_2 + 2C_9 x = 0, \tag{24a}$$

$$(h_1 + h_2)\{2C_4 h_1 - C_5 x\} - \{C_1 - C_2 x + C_4 h_1^2 - C_5 h_1 x + C_6 x^2 + C_7 h_2^2 - C_8 h_2 x + C_9 x^2\} = 0, \tag{24b}$$

$$(h_1 + h_2)(2C_7 h_2 - C_8 x) - \{C_1 - C_2 x + C_4 h_1^2 - C_5 h_1 x + C_6 x^2 + C_7 h_2^2 - C_8 h_2 x + C_9 x^2\} = 0. \tag{24c}$$

Solving equations (24) numerically, the three parameters can be computed and the mean crushing force in equation (22) is determined.

The eccentricity parameters related to each half-wave length are

$$m_1 = \frac{x}{h_1}\cos\alpha\,, \tag{25a}$$

$$m_2 = \frac{x}{h_2}\cos\alpha\,. \tag{25b}$$

The same procedure can be applied for the first fold (or lobe), in which no plastic hinge is formed at the smaller end of the frustum, see Fig. 2. The energy dissipated due to plastic bending becomes:

$$W_B = \int_{\beta=0}^{\frac{\pi}{2}-\alpha} \pi D_B M_p \,\mathrm{d}\beta + \int_{\gamma=0}^{\frac{\pi}{2}+\alpha} \pi (D_B + D_C) M_p \,\mathrm{d}\gamma$$
$$= \frac{\pi Y t^2}{4\sqrt{3}}\{D(3\pi + 2\alpha) - x\{(3\pi + 2\alpha)\cos\alpha + 8\sin\alpha(1 + \sin\alpha)\} + 4(h_1 + h_2)\{\cos\alpha + (\pi + 2\alpha)\sin\alpha\}\}$$

and that due to stretching is the same as:

$$W_S = \pi Y t\{h_1^2(1 - \sin\alpha) - 2h_1 x\cos\alpha + 2x^2(1 + \sin\alpha) + (1 + \sin\alpha)\left(h_2^2 - 2h_2 x\cos\alpha + 2x^2\cos^2\alpha\right)\}.$$

Thus

$$\overline{P} = \frac{1}{(h_1 + h_2)\cos\alpha}\left[\frac{\pi Y t^2}{4\sqrt{3}}\{D(3\pi + 2\alpha) - x\{(3\pi + 2\alpha)\cos\alpha + 8\sin\alpha(1 + \sin\alpha)\} + 4(h_1 + h_2)\{\cos\alpha + (\pi + 2\alpha)\sin\alpha\}\} + \pi Y t\{h_1^2(1 - \sin\alpha) - 2h_1 x\cos\alpha + 2x^2(1 + \sin\alpha) + (1 + \sin\alpha)\left(h_2^2 - 2h_2 x\cos\alpha + 2x^2\cos^2\alpha\right)\}\right]$$
$$= \frac{C_1 - C_2 x + C_3(h_1 + h_2) + C_4 h_1^2 - C_5 h_1 x + C_6 x^2 + C_7 h_2^2 - C_8 h_2 x + C_9 x^2}{h_1 + h_2}$$

where

$$C_1 = \frac{\pi Y t^2 D}{4\sqrt{3}\cos\alpha}(3\pi + 2\alpha),$$

$$C_2 = \frac{\pi Y t^2}{4\sqrt{3}}\{(3\pi + 2\alpha) + 8(1 + \sin\alpha)\tan\alpha\},$$

$$C_3 = \frac{\pi Y t^2}{\sqrt{3}}\{1 + (\pi + 2\alpha)\tan\alpha\},$$

$$C_4 = \frac{\pi Y t}{\cos\alpha}(1 - \sin\alpha), \qquad C_5 = 2\pi Y t,$$

$$C_6 = \frac{2\pi Y t}{\cos\alpha}(1 + \sin\alpha), \qquad C_7 = \frac{\pi Y t}{\cos\alpha}(1 + \sin\alpha),$$

$$C_8 = 2\pi Y t(1 + \sin\alpha), \qquad C_9 = 2\pi Y t(1 + \sin\alpha)\cos\alpha.$$

3. Numerical study

In order to anticipate the inward folding (or lateral deflection) of thin tubes under axial compressive load and verify the theoretical results, ABAQUS 14-2 implicit finite element software was employed for this task with one step analysis. The material properties of the thin tube which used in this model are considered as elastoplastic materials, using isotropic elasticity, standard von Mises yield criterion and an associated flow rule; with yield strength $\sigma_y = 300$ MPa, mass density, $\rho = 7830$ kg/m^3, Poisson's ratio, $\nu = 0.3$, modulus of elasticity, $E = 207$ GPa, and linear hardening modulus of 1000 MPa. This tube is simulated as a 3-D thin shell part with different angle of frustum (between 0 to 25.8 degree). As the main factor of this study is D/t, different values of D/t were studied. The ratio of D/t as taken between 20 to 80. The model consists of three parts: upper surface, lower surface, and the thin tube placed between these surfaces. The two surfaces were modeled as rigid bodies to eliminate their stresses and deflections. The lower surface is totally fixed while the upper surface is allowed to move vertically in z-direction along the tube length as shown in Fig. 3. The upper rigid surface has been given an 80 mm displacement in z-direction with 1 sec time.

For purpose of determining a proper mesh size that gives accurate results and allows reducing the required CPU time, different mesh sizes were analyzed as shown in Fig. 4. In this figure, the value of lateral deflection was linear after 3 mm mesh size. Thus a 3 mm mesh size (2772) elements a 4-node doubly curved thin or thick shell, reduced integration (S4R) was selected for this model. However, a 4-node 3-D bilinear rigid quadrilateral (R3D4) element type was selected for the two rigid surfaces. As the surface contact is not specified, a general contact has been assumed between all surfaces. This includes the contact between upper and lower surfaces with the cylinder and also between all surfaces of generated folds.

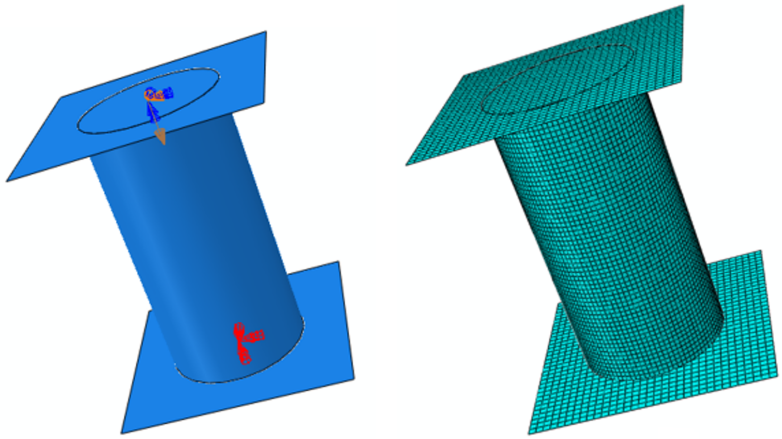

Fig. 3. 3D modeling and mesh model of the crushing process

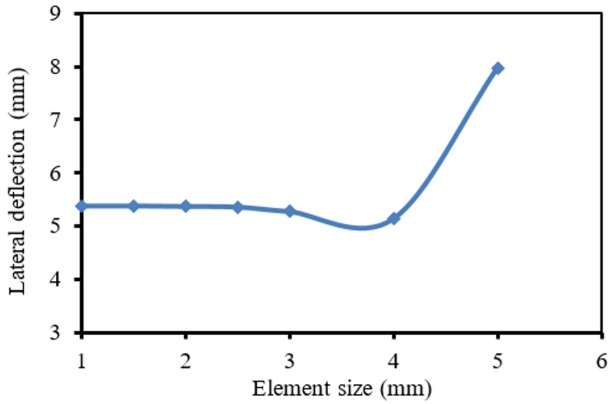

Fig. 4. Mesh sensitivity curve of buckling process

4. Results and discussion

Special cases are examined as follows:

i. Setting $x = 0$, equations ((24b) and (24c)) are reduced to

$$2C_4h_1\,(h_1 + h_2) - \left(C_1 + C_4h_1^2 + C_7h_2^2\right) = 0, \tag{26a}$$

$$2C_7h_2\,(h_1 + h_2) - \left(C_1 + C_4h_1^2 + C_7h_2^2\right) = 0 \tag{26b}$$

which in turn are solved as equations (3) reported by Mamalis et al. [12].

ii. Setting $\alpha = 0$, equations (24) are reduced to

$$h = h_1 = h_2 = 2x - \frac{\pi t}{4\sqrt{3}}, \tag{27a}$$

$$2h^2 - \frac{\pi t D}{\sqrt{3}} + \frac{\pi t}{\sqrt{3}}x - 4x^2 = 0. \tag{27b}$$

Solving equation (27) for x and h,

$$x = \frac{\pi t}{8\sqrt{3}} + \sqrt{\frac{\pi D t}{4\sqrt{3}} - \left[\frac{\pi t}{8\sqrt{3}}\right]^2}, \tag{28a}$$

$$\frac{h}{2} = \sqrt{\frac{\pi D t}{4\sqrt{3}} - \left[\frac{\pi t}{8\sqrt{3}}\right]^2}. \tag{28b}$$

From equation (25), the eccentricity parameter is:

$$m = m_1 = m_2 = \frac{x}{h} = \frac{1}{2} + \frac{1}{\sqrt{\frac{64\sqrt{3}}{\pi}\frac{D}{t} - 4}}. \tag{29}$$

Equation (29) suggests plotting the theoretical together with numerical values of the eccentricity parameter vs. D/t ratio for different values of semi-apical angle of the frusta. Simulations of the axial buckling of frusta having different semi-apical angles are conducted to verify this dependency. A typical example of the simulations is shown in Fig. 5 for the case of cylinder. In Fig. 6, the numerical simulation always underestimates the value of the eccentricity parameter, although with a trend similar to that of theoretical analysis. This underestimation may be attributed to the pre-assumed straight folds used in the analysis, rather than the semi-circle folds actually produced in experiments. The higher the apex angle of a frustum and/or the D/t ratio, the more underestimating is the numerical simulation.

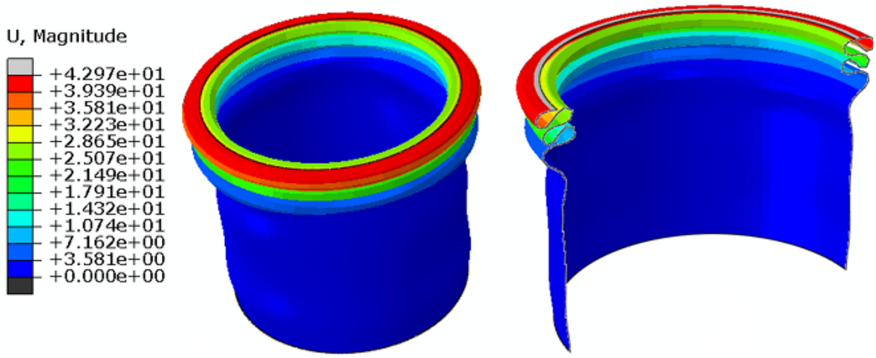

Fig. 5. 3D modeling of the crushing process and cross section of the model

In frusta with high apical angle, the mode of deformation is normally transiting from folding to inversion; Actually, beyond approximately 30°, the present simulation exhibited global inversion of the frusta, although higher values of 45° and 60° were reported by Gupta et al. [14] and Alghamdi et al. [15], respectively.

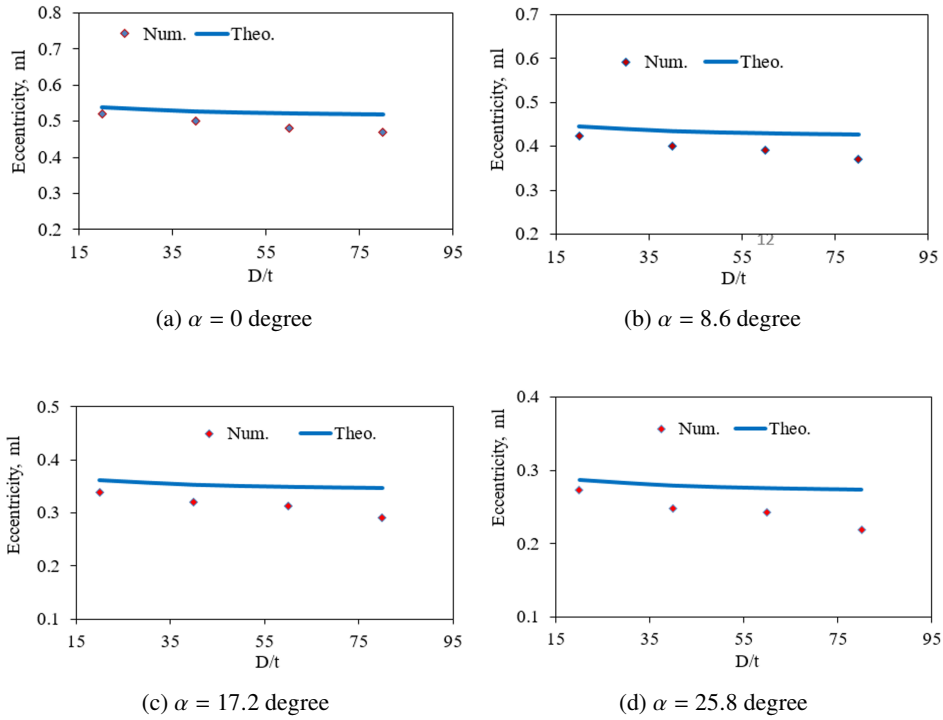

(a) α = 0 degree

(b) α = 8.6 degree

(c) α = 17.2 degree

(d) α = 25.8 degree

Fig. 6. Eccentricity parameter for cylinders

In view of the meagre literature on the topic of inward folding, the present analysis was compared with previous experimental work in Fig. 6, although an extensive oncoming experimental program will be performed for full comprehension of the inward folding mechanism as well as for comparison purposes.

Fig. 7 displays the values of the eccentricity parameter deduced presently from equation (29) and compared with those measured experimentally by Singace et al. [10] as well as the theoretical values estimated by Singace et al. [10]. In view of the inadequate experimental data, especially for other higher D/t ratios associated with the concertina mode of failure, it is fair to conclude that these experimental data are satisfactorily encompassed by the two theories. It should be stated that the theoretical estimate of Singace et al. [10] is constant at $m = 0.65$, irrespective of D/t ratio; a trend which is not followed by experimental data. Further experimentation is thus needed.

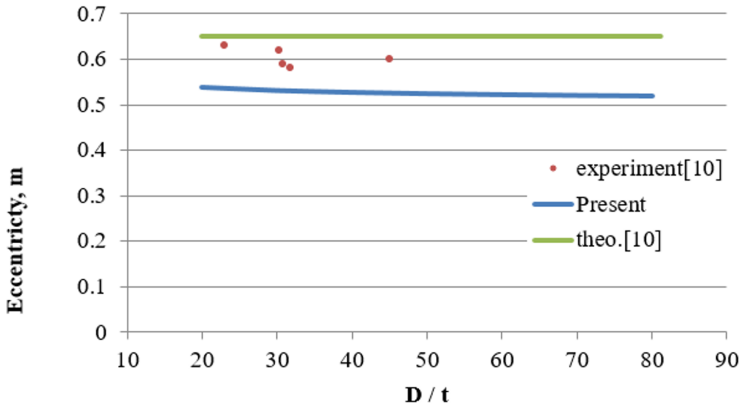

Fig. 7. Eccentricity parameter for cylinders

5. Conclusions

An eccentricity (with reference to the tube generator) relating the inward and outward parts of the folds exists both in cylinders and frusta. While there is little information regarding this topic in cylinders, almost no mention was made for frusta whatsoever. A new model wherein an analysis of the inward folding produced in the axial crushing of frusta was presently built and compared with previous relevant models as well as experimental findings. The present model was substantiated by its flexibility and capability of describing and estimating the inward folding in frusta in general as well as in cylinders as a special case. The analysis suggests a declining trend of the eccentricity dependence with the D/t ratio in contrast with a previous theory which suggested a total independency. Numerical simulations of the process were found to:

- underestimate the theoretical values of inward folding in general,
- anticipate more underestimations as the tubes become thinner and/or have larger apex angle, and
- anticipate as low as 300 apical angle frusta to revert its mode of deformation to global inversion.

References

[1] F.C. Bardi and S. Kyriakides. Plastic buckling of circular tubes under axial compression—part I: Experiments. *International Journal of Mechanical Sciences*, 48(8):830–841, 2006. doi: 10.1016/j.ijmecsci.2006.03.005.

[2] J.M. Alexander. An approximate analysis of the collapse of thin cylindrical shells under axial loading. *The Quarterly Journal of Mechanics and Applied Mathematics*, 13(1):10–15, 1960. doi: 10.1093/qjmam/13.1.10.

[3] A.A.K. Mohammed, M.N. Alam, and R. Ansari. Quasi-static study of thin aluminium frusta with linearly varying wall-thickness. *International Journal of Crashworthiness*, 25(5):473–484, 2020. doi: 10.1080/13588265.2019.1613762.

[4] A. Shiravand and M. Asgari. Hybrid metal-composite conical tubes for energy absorption; theoretical development and numerical simulation. *Thin-Walled Structures*, 145:106442, 2019. doi: 10.1016/j.tws.2019.106442.

[5] P. Sadjad, E.M. Hossein, and E.M. Sobhan. Crashworthiness of double-cell conical tubes with different cross sections subjected to dynamic axial and oblique loads. *Journal of Central South University*, 25:632–645, 2018. doi: 10.1007/s11771-018-3766-z.

[6] G. Lu , J.L. Yu , J.J. Zhang, and T.X. Yu. Alexander revisited: upper- and lower-bound approaches for axial crushing of a circular tube. *International Journal of Mechanical Sciences*, 206:106610, 2021. doi: 10.1016/j.ijmecsci.2021.106610.

[7] A. Sadighi, A. Eyvazian, M. Asgari, and A.M. Hamouda. A novel axially half corrugated thin-walled tube for energy absorption under axial loading. *Thin-Walled Structures*, 145:106418, 2019. doi: 10.1016/j.tws.2019.106418.

[8] M.Y. Abbood, and R.N. Kiter. On the peak quasi-static load of axisymmetric buckling of circular tubes. *International Journal of Crashworthiness*, 27(2):367–375, 2022. doi: 10.1080/13588265.2020.1807679.

[9] T. Wierzbicki, S.U. Bhat, W. Abramowicz, and D. Brodkin. Alexander revisited—A two folding elements model of progressive crushing of tubes. *International Journal of Solids and Structures*, 29(4):3269–3288, 1992. doi: 10.1016/0020-7683(92)90040-Z.

[10] A.A. Singace, H. Elsobky, and T.Y. Reddy. On the eccentricity factor in the progressive crushing of tubes. *International Journal of Solids and Structures*, 32(24):3589-3602, 1995. doi: 10.1016/0020-7683(95)00020-B.

[11] H.E. Postlethwaite and B. Mills. Use of collapsible structural elements as impact isolators, with special reference to automotive applications. *The Journal of Strain Analysis for Engineering Design*, 5(1):58–73,1970. doi: 10.1243/03093247V051058.

[12] A.G. Mamalis, D.E. Manolakos, S. Saigal, G. Viegelahn, and W. Johnson. Extensible plastic collapse of thin-wall frusta as energy absorbers. *International Journal of Mechanical Sciences*, 28(4):219–229, 1986. doi: 10.1016/0020-7403(86)90070-6.

[13] A.G. Mamalis, D.E. Manolakos, G.L. Viegelahn, and W. Johnson. The modeling of the progressive extensible plastic collapse of thin-wall shells. *International Journal of Mechanical Sciences*, 30(3-4):249–261, 1988. doi: 10.1016/0020-7403(88)90058-6.

[14] N.K. Gupta, G.L. Prasad, and S.K. Gupta. Plastic collapse of metallic conical frusta of large semi-apical angles. *International Journal of Crashworthiness*, 2(4):349–366, 1997. doi: 10.1533/cras.1997.0054.

[15] A.A.A. Alghamdi, A.A.N. Aljawi, and T.M.N. Abu-Mansour. Modes of axial collapse of unconstrained capped frusta. *International Journal of Mechanical Sciences*, 44(6):1145–1161, 2002. doi: 10.1016/S0020-7403(02)00018-8.

[16] N.M. Sheriff, N.K. Gupta, R. Velmurugan, and N. Shanmugapriyan. Optimization of thin conical frusta for impact energy absorption. *Thin-Walled Structures*, 46(6):653–666, 2008. doi: 10.1016/j.tws.2007.12.001.